DMD Fast Forward. Published on April 13, 2009 as doi:10.1124/dmd.108.026062

Prediction of the hepatic and renal clearance of transporter substrates in rats using in vitro uptake experiments

Tomoko Watanabe, Kazuya Maeda, Tsunenori Kondo, Hideki Nakayama, Shigeru Horita, Hiroyuki Kusuhara and Yuichi Sugiyama

Department of Molecular Pharmacokinetics, Graduate School of Pharmaceutical Sciences, The University of Tokyo, Japan (T.W., K.M., H.K., Y.S.)

Department of Urology, Kidney Center, Tokyo Women's Medical University, Tokyo, Japan (T.K., H.N., S.H.)

DMD Fast Forward. Published on April 13, 2009 as DOI: 10.1124/dmd.108.026062
This article has not been copyedited and formatted. The final version may differ from this version.

Running title: Prediction of hepatic and renal clearance from uptake assay

Corresponding author: Yuichi Sugiyama, Ph.D.

Address: Department of Molecular Pharmacokinetics, Graduate School of Pharmaceutical Sciences, The University of Tokyo, 7-3-1 Hongo, Bunkyo-ku, Tokyo, 113-0033, Japan

Phone: +81-3-5841-4770, *Fax*: +81-3-5841-4766

E-mail: sugiyama@mol.f.u-tokyo.ac.jp

The number of text pages: 31

The number of Figures: 5

The number of Tables: 5

The number of references: 32

The number of words in Abstract: 240 words, Introduction: 729 words, and Discussion: 1489 words

Abbreviations: Oatp, organic anion transporting polypeptide; Oat, organic anion transporter; AUC, area under the plasma concentration–time profile; SD, Sprague Dawley; PCG, benzylpenicillin; LC/MS, liquid chromatography/mass spectrometry.

Abstract

The clearance route and the absolute values for hepatic and renal clearance of drugs are important criteria for the selection of drug candidates. Based on pharmacokinetic theory, assuming that uptake is the rate-determining process for the biliary excretion of drugs, organ intrinsic clearance should be simply estimated by the intrinsic uptake. In this study, to investigate whether organ clearance can be predicted from the in vitro uptake activity, we performed the uptake experiments using isolated hepatocytes and kidney slices, integration plot analyses, and in vivo pharmacokinetic studies using 12 barely metabolized drugs in rats. The in vivo hepatic and renal clearance could be approximated by uptake clearance estimated from integration plot analyses, except for the renal clearance of some drugs that was relatively small. The comparison of intrinsic uptake clearance from in vitro experiments and integration plot studies revealed that in vivo hepatic uptake was well explained by uptake into isolated hepatocytes, while in kidney, in vivo uptake clearance was 10 to 100 times that in kidney slices and a scaling factor is required for its prediction from in vitro experiments. The organ clearance and the fraction excreted into urine could be predicted from in vitro studies except for drugs whose renal clearance was relatively small. This study suggests that the uptake process is the determining factor for organ clearance of minimally metabolized drugs, and uptake assays using isolated hepatocytes and kidney slices are useful for evaluating the uptake clearance.

DMD Fast Forward. Published on April 13, 2009 as DOI: 10.1124/dmd.108.026062
This article has not been copyedited and formatted. The final version may differ from this version.

Introduction

To select drug candidates rationally in the early stage of drug development, many characteristics of the drugs should be taken into account. The pharmacokinetic property of drugs determine their systemic exposure and local distribution, and thus it is an important factor for optimizing the pharmacological and toxicological effects. It is determined by several intrinsic factors such as metabolism, membrane transport and protein binding, and various in vitro experimental systems have been established (Roberts, 2001; Balani et al., 2005).

Drugs are mainly cleared from the blood circulation by the liver and kidney, and many kinds of metabolic enzymes and transporters are responsible for their elimination (Ito et al., 2005; Shitara et al., 2006). The relative contribution of the liver and kidney to the overall clearance of drugs is important for considering their pharmacological and toxicological effects. Much evidence has indicated that the function of metabolic enzymes and transporters is modified by several factors such as pathophysiological conditions, genetic polymorphisms, and drug-drug interactions (Shitara et al., 2005; Ieiri et al., 2006; Konig et al., 2006; Shitara et al., 2006; Lynch and Price, 2007). Therefore, to avoid large changes in the pharmacokinetics of drugs in unusual circumstances, clearance from multiple elimination pathways in liver and kidney is thought to be a desirable feature for many drugs. For example, the plasma concentration of enalaprilat was significantly increased by reduced renal function, whereas that of temocaprilat was not significantly changed (Oguchi et al., 1993) because enalaprilat is predominantly excreted from the kidney, while temocaprilat is excreted from both the liver and kidney, which can minimize the effect of renal dysfunction because of its alternative elimination route by the liver (Ishizuka et al., 1997; Ishizuka et al., 1998). On the other hand, if the pharmacological target is the liver or kidney, efficient targeting of drugs is needed to maximize the pharmacological effect. Pravastatin, a hydrophilic HMG-CoA reductase inhibitor, is efficiently retained in the enterohepatic circulation, which enables the long-term inhibition of HMG-CoA reductase in liver and the avoidance of its systemic side effects such as myopathy (Kitamura et al., 2008a). Antibiotics excreted mainly into bile and urine are selected for the treatment of bile duct inflammation and infection of the urinary tract, respectively (Tsuji, 2006). Thus, the prediction of the elimination route of

DMD Fast Forward. Published on April 13, 2009 as DOI: 10.1124/dmd.108.026062
This article has not been copyedited and formatted. The final version may differ from this version.

drugs is essential for the development of desirable drugs. However, in vitro experimental systems for its prediction have not been established yet.

Apparent intrinsic clearance ($CL_{int,app}$) consists of (1) uptake clearance from blood to an organ (P_1), (2) backflux clearance from the organ to the blood (P_2), and (3) metabolism, or biliary or urinary excretion (P_3), and can be described as the following equation (Shitara et al., 2006).

$$CL_{int,app} = P_1 \times \frac{P_3}{P_2 + P_3} \qquad \text{(Eq. 1)}$$

When P_3 is much larger than P_2, apparent intrinsic clearance can approximate intrinsic uptake clearance (P_1). In this case, the uptake clearance is the sole determinant of the overall intrinsic clearance and therefore the hepatic and renal clearance of drugs can be predicted by uptake clearance.

In the process of the hepatic and renal uptake of organic anions, organic anion transporting polypeptide (Oatp) and organic anion transporter (Oat) family transporters, respectively, which are expressed on the basal membrane, are mainly involved (Shitara et al., 2006). For the characterization of uptake properties of drugs in the liver and kidney, isolated hepatocytes and kidney slices can be used (Shitara et al., 2006). Our group previously demonstrated that tissue uptake clearance of several compounds obtained from a multiple indicator dilution method is well explained by the in vitro uptake clearance into isolated hepatocytes (Miyauchi et al., 1993) in rats. Hasegawa et al. have shown that rat kidney slices can be useful for predicting the renal uptake clearance of compounds and the relative contribution of Oat1 and Oat3 to their overall uptake (Hasegawa et al., 2003). These experimental systems can also be directly applied to humans using cryopreserved human hepatocytes and human kidney slices to predict the hepatic and renal uptake clearance (Hirano et al., 2004; Nozaki et al., 2004).

The purpose of this study was to examine whether hepatic and renal clearance could be predicted simply from in vitro uptake studies using isolated hepatocytes and kidney slices in rats using 12 minimally metabolized anionic drugs from four therapeutic categories (HMG-CoA reductase inhibitors, angiotensin II receptor antagonists, angiotensin converting enzyme (ACE) inhibitors, and β-lactam antibiotics), each of which has a different urinary and biliary excreted fraction.

Materials and Methods

Materials. [^{3}H]-Pravastatin (44.6 Ci/mmol), [^{3}H]-olmesartan (79 Ci/mmol) and [^{14}C]-temocaprilat (16.0 mCi/mmol) and unlabeled pravastatin, olmesartan and temocaprilat were kindly donated by Daiichi-Sankyo Co. (Tokyo, Japan). [^{3}H]-Valsartan (81.0 Ci/mmol) and unlabeled valsartan were kindly donated by Novartis Pharma (Basel, Switzerland). [^{3}H]-Pitavastatin (16 Ci/mmol) was kindly donated by Kowa Co. (Tokyo, Japan), and [^{3}H]-rosuvastatin (79 Ci/mmol) by AstraZeneca (London, UK). Unlabeled pitavastatin was synthesized by Nissan Chemical Industries (Chiba, Japan). Unlabeled rosuvastatin, candesartan, and benazeprilat were purchased from Toronto Research Chemicals (North York, Canada). [^{3}H]-Estradiol-17β-glucuronide ($E_2$17βG) (53 Ci/mmol), [^{3}H]-taurocholate (5.0 Ci/mmol), and [^{3}H]-*p*-aminohippurate (PAH) (4.1 Ci/mmol) were purchased from PerkinElmer Life Sciences (Boston, MA). [^{14}C]-Benzylpenicillin (PCG) (59 mCi/mmol) was purchased from GE Healthcare UK (Buckinghamshire, England). Unlabeled $E_2$17βG, taurocholate, PAH, ceftizoxime and cefmetazole were purchased from Sigma-Aldrich (St. Louis, MO). Unlabeled PCG and enalaprilat were purchased from Wako Pure Chemicals (Osaka, Japan). All other chemicals were of analytical grade and commercially available.

Animals. Female Sprague Dawley (SD) rats (6–7 weeks old) were purchased from Nippon SLC (Shizuoka, Japan). All animals were maintained under standard conditions with a reverse dark–light cycle and were treated humanely. Food and water were available ad libitum. The studies reported in this manuscript were conducted in accordance with the guidelines provided by the Institutional Animal Care Committee (Graduate School of Pharmaceutical Sciences, The University of Tokyo, Tokyo, Japan).

In vivo pharmacokinetic study. Female SD rats weighing approximately 170 to 200 g were used for these experiments. Under light ether anesthesia, their femoral artery and vein were cannulated with polyethylene catheters (SP-31; Natsume Seisakusyo, Tokyo, Japan), the bile duct was cannulated with a polyethylene catheter (PE-10; Natsume Seisakusyo) for bile collection, and the bladder was cannulated with a polyethylene tube for urine collection. After the surgical procedures, the rats were placed in a restraining cage (Ballman cage; Natsume Seisakusyo) and allowed to recover from the anesthesia. The rats received a bolus intravenous administration of pitavastatin (0.2 mg/kg), rosuvastatin (0.5 mg/kg), valsartan

DMD Fast Forward. Published on April 13, 2009 as DOI: 10.1124/dmd.108.026062
This article has not been copyedited and formatted. The final version may differ from this version.

(0.5 mg/kg), olmesartan (0.08 mg/kg), candesartan (0.08 mg/kg), temocaprilat (0.5 mg/kg), enalaprilat (0.5 mg/kg), benazeprilat (0.5 mg/kg), PCG (2 mg/kg), or ceftizoxime (1 mg/kg), or constant infusion of pravastatin (76 mg/min/kg after bolus intravenous administration of 0.67 mg/kg), or cefmetazole (0.1 mg/min/kg) into their femoral vein. Blood samples were collected from the femoral artery at designated times. Bile and urine were collected in preweighed test tubes at designated times. Plasma was prepared by centrifugation of the blood samples (15,000 *g*, 5 min, Microfuge; Beckman Coulter). All samples were stored at –20°C until drug concentrations were measured by LC/MS.

Integration plot analysis. Female SD rats weighing approximately 170 to 200 g were used for these experiments. Under light ether anesthesia, their femoral artery and vein were cannulated with polyethylene catheters (SP-31; Natsume Seisakusyo). The rats received a bolus intravenous administration of pravastatin (0.1 mg/kg), pitavastatin (0.2 mg/kg), rosuvastatin (0.05 mg/kg), valsartan (0.01 mg/kg), olmesartan (0.02 mg/kg), candesartan (0.02 mg/kg), temocaprilat (0.01 mg/kg), enalaprilat (0.5 mg/kg), benazeprilat (0.5 mg/kg), PCG (1 mg/kg), ceftizoxime (1 mg/kg), or cefmetazole (2 mg/kg). Blood samples were collected from the femoral artery at 15, 30, 45, 60, 90, and 120 s. The rats were sacrificed at 30, 60, or 120 s after dosing, and their liver and kidney were immediately removed. Plasma was prepared by centrifugation of the blood samples (15,000 *g*, 5 min, Microfuge; Beckman Coulter). PBS was added to tissue samples and homogenized to make a 30% homogenate. All samples were stored at –20°C until drug concentrations were measured by LC/MS.

Determination of the plasma protein-unbound fraction (f_u) and blood-to-plasma concentration ratio (R_B). Binding of drugs to plasma proteins was determined by an ultrafiltration method. Plasma was obtained by the centrifugation of blood from female SD rats. Drugs were individually added to the plasma samples and they were incubated together at 37°C for 5 min. Following the manufacturer's protocol, the specimen was directly applied to Centrifree micropartition devices (Millipore Corporation, Bedford, MA). The concentrations of the drugs in the filtrate and the plasma before filtration were determined by LC/MS. The adsorption of the drugs on the membrane was confirmed to be negligible.

DMD Fast Forward. Published on April 13, 2009 as DOI: 10.1124/dmd.108.026062
This article has not been copyedited and formatted. The final version may differ from this version.

To determine the R_B values, blood was obtained from female SD rats. Drugs were individually added to the blood samples and they were incubated together at 37°C for 5 min. Plasma was prepared by centrifugation of the blood samples (15,000 *g*, 5 min, Microfuge; Beckman Coulter). The concentrations of the drugs in the blood and the plasma samples were determined by LC/MS.

The protein-unbound fraction in the blood (f_B) was calculated by dividing the protein-unbound fraction in plasma (f_u) by R_B.

Uptake study using rat freshly isolated hepatocytes. Isolation of hepatocytes and an uptake study were conducted as described previously (Yamazaki et al., 1993). Isolated hepatocytes (viability > 85%) were suspended in Krebs–Henseleit buffer (118 mM NaCl, 23.8 mM $NaHCO_3$, 4.8 mM KCl, 1.0 mM KH_2PO_4, 1.2 mM $MgSO_4$, 12.5 mM HEPES, 5.0 mM glucose, 1.5 mM $CaCl_2$, pH 7.4) and stored on ice. Before the uptake study, hepatocytes were preincubated at 37°C for 3 min and the uptake reaction was started by adding drugs to the hepatocyte suspension. After a designated time, the reaction was terminated by separating the cells from the medium using a centrifugal filtration technique. For this purpose, a 100 μL aliquot of incubation mixture was placed in a 0.4 mL centrifuge tube (Sarstedt, Numbrecht, Germany) containing 50 μL of 2N sodium hydroxide for radiolabeled compounds or 100 μL of 5M sodium acetate for unlabeled compounds under a 100 μL layer of an oil mixture (density, 1.05; mixture of silicone oil and mineral oil, Sigma-Aldrich). Samples were then centrifuged for 10 s in a Microfuge (Beckman Coulter, Fullerton, CA). During this process, the hepatocytes pass through the oil layer into the aqueous solution (2N NaOH or 5M CH_3COONa). In the case of unlabeled compounds, tubes were frozen in liquid nitrogen immediately after centrifugation and stored at –20°C until drug measurement.

The concentrations of pravastatin, pitavastatin, rosuvastatin, valsartan, olmesartan, temocaprilat, PCG, $E_2$17βG, and taurocholate were determined by measuring their radioactivity. After overnight incubation at room temperature to dissolve the cells in alkali, the centrifuge tube was cut and each compartment was transferred to a scintillation vial. The compartment containing dissolved cells was neutralized with 50 μL of 2N hydrochloric acid, mixed with scintillation cocktail (Clearsol II; Nakalai Tesque, Kyoto, Japan), and the radioactivity was determined in a liquid scintillation counter (LS6000SE; Beckman Coulter). The concentrations of candesartan, benazeprilat, enalaprilat, ceftizoxime, and cefmetazole were determined by

LC/MS. Cells in 5M sodium acetate buffer were taken from the centrifuge tube and sonicated in a new tube to break them down. This sample was used for the measurement of drug concentrations by LC/MS.

Uptake study using rat kidney slices. An uptake study using rat kidney slices was conducted as described previously (Hasegawa et al., 2002). Kidney slices (300 μm thick) from female SD rats were kept in ice-cold buffer (120 mM NaCl, 16.2 mM KCl, 1 mM $CaCl_2$, 1.2 mM $MgSO_4$ in 10 mM NaH_2PO_4/Na_2HPO_4, pH 7.5). Two slices, each weighing 15 to 25 mg, were randomly selected and then incubated in each well of a 12-well plate with 1 mL of oxygenated buffer after preincubation of slices for 5 min at 37°C. After incubating for designated periods, each slice was rapidly removed from the incubation buffer, washed with ice-cold buffer, blotted on filter paper and weighed.

The concentrations of pravastatin, pitavastatin, rosuvastatin, valsartan, olmesartan, temocaprilat, PCG, and PAH were determined by measuring their radioactivity. The slice was dissolved in 1 mL of Soluene-350 (Perkin Elmer Life Science). The radioactivity in scintillation cocktail (Hionic-Fluor; Perkin Elmer Life Sciences) was determined by liquid scintillation counting (LS6000SE; Beckman Coulter). The concentrations of candesartan, benazeprilat, enalaprilat, ceftizoxime, and cefmetazole were determined by LC/MS. PBS (100 μL) was added to the slices followed by sonication to break them down. This sample was used for the measurement of drug concentration by LC/MS.

Quantification of drug concentration by LC/MS. Samples were precipitated with three volumes of acetonitrile (for in vivo samples and kidney slices) or methanol (for hepatocytes) and centrifuged at 15,000 *g* at 4°C for 10 min. The supernatants were subjected to LC/MS. LCMS-2010 EV equipped with a Prominence LC system (Shimadzu, Kyoto, Japan), an Alliance HT 2795 separation module with an autosampler (Waters, Milford, MA), and a Micromass ZQ mass spectrometer with an electron ion spray interface (Waters) were used. In the measurement using Shimadzu equipment, the interface voltage was 3.5 kV, and the nebulizer gas (N_2) flow was 1.5 L/min. The heat block and curved desolvation line temperatures were 200°C and 150°C, respectively. In the measurement using Waters equipment, the desolvation temperature was 350°C and the capillary voltage was 3.8 kV. Detailed conditions for the measurement of each compound are shown in the supplemental data (Table S1).

DMD Fast Forward. Published on April 13, 2009 as DOI: 10.1124/dmd.108.026062
This article has not been copyedited and formatted. The final version may differ from this version.

Pharmacokinetic analysis.

In vivo study

The area under the plasma concentration-time profile over 120 min ($AUC_{0–120}$) was calculated using a trapezoidal method. The plasma concentration–time profile was fitted to the two exponential equations using a nonlinear iterative least squares method using MULTI software (Yamaoka et al., 1981) and $AUC_{0–\infty}$ was estimated by integration of the fitted equation from time 0 to infinity. The plasma clearance ($CL_{tot,p}$), the biliary clearance based on the drug concentration in plasma ($CL_{bile,p}$), and the renal clearance based on the drug concentration in plasma ($CL_{renal,p}$) were calculated using the following equations:

$$CL_{tot,p} = \frac{Dose}{AUC_{0-\infty}}, \quad \text{(Eq. 2)}$$

$$CL_{bile,p} = \frac{X_{bile}}{AUC_{0-120}}, \quad \text{(Eq. 3)}$$

$$CL_{renal,p} = \frac{X_{urine}}{AUC_{0-120}}, \quad \text{(Eq. 4)}$$

where X_{bile} represents the cumulative excreted amount in bile over 120 min and X_{urine} represents the amount in urine over 120 min.

When the drugs were infused intravenously, $CL_{tot,p}$, $CL_{bile,p}$, and $CL_{renal,p}$ were calculated using the following equations:

$$CL_{tot,p} = \frac{I}{C_{pss}}, \quad \text{(Eq. 5)}$$

$$CL_{bile,p} = \frac{V_{bile}}{C_{pss}}, \quad \text{(Eq. 6)}$$

$$CL_{renal,p} = \frac{V_{urine}}{C_{pss}}, \quad \text{(Eq. 7)}$$

DMD Fast Forward. Published on April 13, 2009 as DOI: 10.1124/dmd.108.026062
This article has not been copyedited and formatted. The final version may differ from this version.

where *I* represents the infusion rate, C_{pss} the drug concentration in plasma at steady state, V_{bile} the biliary excretion rate at steady state, and V_{urine} the urinary excretion rate at steady state. C_{pss} was determined as the mean value of the plasma concentration at 30, 60, 90, and 120 min. V_{bile} and V_{urine} were determined as the mean value of the renal excretion rate from 30–60 min, 60–90 min, and 90–120 min. The clearances based on drug concentration in whole blood ($CL_{tot,B}$, $CL_{bile,B}$, and $CL_{renal,B}$) were calculated by dividing $CL_{tot,p}$, $CL_{bile,p}$ and $CL_{renal,p}$ by R_B, respectively.

Integration plot analysis

The AUC_{0-t} was calculated using a trapezoidal method. The tissue uptake amount of drugs per g tissue (X_t) normalized by the plasma concentration (C_p) can be described as the following equation:

$$\frac{X_t(t)}{C_p(t)} = CL_{uptake,p} \times \frac{AUC_{0-t}}{C_p(t)} + \frac{X_t(0)}{C_p(0)} \qquad \text{(Eq. 8)}$$

where $CL_{uptake,p}$ represents tissue uptake clearance based on the drug concentration in plasma and $X_t(0)/C_p(0)$ represents the initial distribution volume. Based on Equation 8, the $AUC_{0-t}/C_p(t)$ value was plotted against $X_t(t)/C_p(t)$ value and each plot was fitted to the straight line using a nonlinear iterative least squares method. $CL_{uptake,p}$ was obtained as a slope of the fitted line. The uptake clearance based on drug concentration in whole blood ($CL_{uptake,B}$) was calculated by dividing $CL_{uptake,p}$ by R_B. Because renal clearance includes glomerular filtration and tubular secretion in the kidney, the tubular secretion clearance, which corresponds to in vitro uptake clearance in kidney slices, was estimated by subtracting $f_B \times$ GFR (glomerular filtration rate; 12 mL/min/kg) from $CL_{uptake,B}$.

In the dispersion model, organ clearance (CL_{org}) is expressed as a function of the intrinsic clearance (CL_{int}), organ blood flow rate (Q), f_B, and dispersion number (D_N).

$$CL_{org} = Q \times (1 - F) \qquad \text{(Eq. 9)}$$

$$F = \frac{4a}{(1+a)^2 \cdot \exp\{(a-1)/2D_N\} - (1-a)^2 \cdot \exp\{-(a+1)/2D_N\}} \qquad \text{(Eq. 10)}$$

DMD Fast Forward. Published on April 13, 2009 as DOI: 10.1124/dmd.108.026062
This article has not been copyedited and formatted. The final version may differ from this version.

$$a = (1 + 4R_N \cdot D_N)^{1/2} \quad \text{(Eq. 11)}$$

$$R_N = f_B \cdot \frac{CL_{int}}{Q} \quad \text{(Eq. 12)}$$

The blood flow rate in the liver was set at 60 mL/min/kg and at 40 mL/min/kg in the kidney (Davies and Morris, 1993), and D_N was set at 0.17 (Roberts and Rowland, 1986; Iwatsubo et al., 1996). Because the in vivo intrinsic uptake clearance from blood to tissue ($P_{1,vivo}$) can be regarded as the organ intrinsic clearance (CL_{int}) when the rate-limiting step of the overall clearance is the uptake process, $P_{1,vivo}$ (= CL_{int}) was calculated by assigning $CL_{uptake,B}$ value to the CL_{org} in Equations 9–12. When calculating $P_{1,vivo}$ values, drugs whose clearance was close to the blood flow (extraction ratio > 0.7) were excluded because we cannot obtain the accurate $P_{1,vivo}$ value. The detailed calculation procedures of the parameters for the in vivo uptake clearance of valsartan as an example can be found in the supplemental data (Appendix and supplemental figure (Fig. S1)).

In vitro studies

The in vitro intrinsic uptake clearance ($P_{1,vitro}$) was calculated by dividing initial uptake velocity by the drug concentration in the incubation buffer. The initial uptake velocity of the drugs was calculated as a slope of the uptake volume at 0.5 and 1 min in isolated hepatocytes, and at 5 min and 10 min in kidney slices. CL_{org} was calculated based on Equations 9–12, assuming that $P_{1,vitro}$ was equal to CL_{int}. In the case of liver, the calculated CL_{org} is expressed as the predicted hepatic clearance ($CL_{h,predicted}$). In the case of kidney, the calculated CL_{org} corresponds to the secretion clearance and the predicted renal clearance ($CL_{r,predicted}$) was calculated using the following equation:

$$CL_{r,\,predicted} = CL_{org} + f_B \times GFR\,. \quad \text{(Eq. 13)}$$

The detailed calculation procedures of the pharmacokinetic parameters estimated from in vitro assay of valsartan as an example can be found in the supplemental data (Appendix and supplemental figures (Figs. S2 and S3)).

DMD Fast Forward. Published on April 13, 2009 as DOI: 10.1124/dmd.108.026062
This article has not been copyedited and formatted. The final version may differ from this version.

The predicted value of the fraction excreted into urine ($f_{urine,predicted}$) was calculated using the following equation:

$$f_{urine,\,predicted} = \frac{CL_{r,\,predicted}}{CL_{r,\,predicted} + CL_{h,\,predicted}}. \qquad \text{(Eq. 14)}$$

In the process of in vitro–in vivo scale-up, we used the following parameters: 1.25×10^8 hepatocytes/g liver, 38.3 g liver/kg body weight and 7.27 g kidney/kg body weight.

Simple mathematical model for explaining the relationship between the true intrinsic uptake clearance ($P_{1KID,corrected}$) and observed uptake clearance in kidney slices (P_{1KID})

One of the possible reasons for the discrepancy between predicted and observed intrinsic uptake clearance in the kidney was that the drug concentration inside the cells of kidney slices was lower than that in the buffer because a kidney slice consists of multiple cell layers and drugs cannot easily penetrate the multilayered cells (see also **Results**). Therefore, to explain the relationship between the true intrinsic uptake clearance ($P_{1KID,corrected}$) and the observed uptake clearance in kidney slices (P_{1KID}), we constructed the simple mathematical model as shown in Figure 1.

We assumed that a kidney slice consists of multiple cell monolayers (the number of monolayers = N), and that V, C_n, and X_n represent the volume of extracellular fluid compartment for each layer, the drug concentration in an extracellular fluid compartment at the n^{th} layer, and the amount of drug taken up into an extracellular fluid compartment at the n^{th} layer. In this model, we assumed that the drug is unidirectionally transported from an extracellular fluid compartment at the n^{th} layer to that at the $(n+1)^{th}$ layer with a clearance of P_2 and that the drug is also taken up into an intracellular compartment at each layer from an extracellular fluid compartment at the same layer with a clearance of P_1'. We also assumed that the drug concentration in an extracellular fluid compartment at the first layer is regarded as that in the incubation medium (set as A).

In this condition, the mass-balance equation for an extracellular fluid compartment at the n^{th} layer (n = 2 ~ (N–1)) can be described as the following equation:

DMD Fast Forward. Published on April 13, 2009 as DOI: 10.1124/dmd.108.026062
This article has not been copyedited and formatted. The final version may differ from this version.

$$V\frac{dC_n}{dt} = P_2 \cdot C_{(n-1)} - (P_1' + P_2) \cdot C_n . \qquad \text{(Eq. 15)}$$

The equation for an extracellular fluid compartment at the Nth layer is as follows:

$$V\frac{dC_N}{dt} = P_2 \cdot C_{(N-1)} - P_1' \cdot C_N . \qquad \text{(Eq. 16)}$$

At the steady state, Equations 15 and 16 can be converted to the following equations:

$$C_n = \frac{P_2}{P_1' + P_2} \cdot C_{(n-1)} = \left(\frac{P_2}{P_1' + P_2}\right)^{n-1} \cdot A \qquad (n = 2 \sim (N-1)), \qquad \text{(Eq. 17)}$$

$$C_N = \frac{P_2}{P_1'} \cdot C_{(N-1)} = \frac{P_2}{P_1'} \cdot \left(\frac{P_2}{P_1' + P_2}\right)^{N-2} \cdot A . \qquad \text{(Eq. 18)}$$

The velocity of drug uptake into an intracellular compartment at the nth layer is as follows:

$$\frac{dX_n}{dt} = P_1' \cdot C_n . \qquad \text{(Eq. 19)}$$

The velocity of drug uptake into the whole kidney slice (v) can be described as the sum of the uptake velocity into an intracellular compartment at each layer.

DMD Fast Forward. Published on April 13, 2009 as DOI: 10.1124/dmd.108.026062
This article has not been copyedited and formatted. The final version may differ from this version.

$$
\begin{aligned}
v &= \sum_{k=1}^{N} \frac{dX_k}{dt} \\
&= \sum_{k=1}^{N} P_1' \cdot C_k \\
&= P_1' \left\{ A + \frac{P_2}{P_1'+P_2} \cdot A + \left(\frac{P_2}{P_1'+P_2} \right)^2 \cdot A + \cdots\cdots + \left(\frac{P_2}{P_1'+P_2} \right)^{N-2} \cdot A + \frac{P_2}{P_1'} \cdot \left(\frac{P_2}{P_1'+P_2} \right)^{N-2} \cdot A \right\} \\
&= P_1' \cdot A \frac{1 - \left(\frac{P_2}{P_1'+P_2} \right)^{N-1}}{1 - \frac{P_2}{P_1'+P_2}} + P_2 \cdot A \left(\frac{P_2}{P_1'+P_2} \right)^{N-2} \\
&= A(P_1'+P_2) \left\{ 1 - \left(\frac{P_2}{P_1'+P_2} \right)^{N-1} \right\} + P_2 \cdot A \left(\frac{P_2}{P_1'+P_2} \right)^{N-2} \\
&= A(P_1'+P_2)
\end{aligned}
$$

(Eq. 20)

Thus, the uptake clearance in the whole kidney slice (P_{1KID}) is shown below.

$$P_{1KID} = \frac{v}{A} = \frac{A(P_1'+P_2)}{A} = P_1'+P_2 \qquad \text{(Eq. 21)}$$

P_1' is defined as the intrinsic uptake clearance for each cell monolayer in a kidney slice, while $P_{1KID,corrected}$ is defined as the "true" intrinsic uptake clearance for the whole kidney slice.

$$P_{1KID,corrected} = N \cdot P_1' \qquad \text{(Eq. 22)}$$

Thus, when assigning Equation 22 to Equation 21, the following equation can be obtained.

$$P_{1KID,corrected} = N \cdot (P_{1KID} - P_2) \qquad \text{(Eq. 23)}$$

Results

Measurement of in vivo organ clearances in rats. The pharmacokinetic parameters for 12 drugs after intravenous administration to female SD rats were calculated and are shown in Table 1. Ten drugs, except for pravastatin and cefmetazole, were administered by intravenous bolus injection. It was thought to be difficult to measure the plasma concentration of pravastatin quantitatively because of its rapid elimination from blood circulation after intravenous bolus administration. It was difficult to measure the plasma concentration of cefmetazole after intravenous bolus administration because of its low sensitivity in LC/MS analysis. Therefore, pravastatin and cefmetazole were administered by constant intravenous infusion. At 120 min after bolus administration or at reaching the steady state in the i.v. infusion study (cefmetazole, pravastatin), more than 80% of the dose was excreted into bile and urine in an unchanged form, except for pitavastatin (64%), suggesting that drugs used in this study were mainly eliminated from the body in an unchanged form in female SD rats. We also measured the plasma protein unbound fraction (f_u) and blood-to-plasma concentration ratio (R_B) of each drug; the results are shown in Table 2.

Measurement of the in vivo tissue uptake clearance obtained from integration plot analyses. To estimate the in vivo tissue uptake clearance of drugs directly, integration plot analyses were performed. The tissue uptake clearance from blood to organ (liver or kidney) was calculated as the slope of the fitted line of the integration plot as described in the **Materials and Methods** section and is shown in Table 3.

Comparison between the organ clearance ($CL_{bile,B}$ and $CL_{renal,B}$) and the tissue uptake clearance ($CL_{uptake,B,liver}$ and $CL_{uptake,B,kidney}$) in vivo. To show the importance of uptake clearance as a determinant factor for organ clearance, the organ clearance ($CL_{bile,B}$ and $CL_{renal,B}$) was compared with the respective tissue uptake clearance ($CL_{uptake,B,liver}$ and $CL_{uptake,B,kidney}$) (Fig. 2). In the liver, $CL_{bile,B}$ values for 6 and 9 of 12 compounds were correlated with $CL_{uptake,B,liver}$ values within a twofold and threefold range of difference, respectively (Fig. 2 (A)). On the other hand, in the kidney, $CL_{renal,B}$ values for 6 and 8 of 12 compounds were correlated with $CL_{uptake,B,kidney}$ values within a twofold and threefold range of difference, respectively,

DMD Fast Forward. Published on April 13, 2009 as DOI: 10.1124/dmd.108.026062
This article has not been copyedited and formatted. The final version may differ from this version.

but $CL_{renal,B}$ values for pitavastatin, valsartan, olmesartan, and candesartan, whose $CL_{renal,B}$ values were relatively small among test compounds, were much smaller than $CL_{uptake,B,kidney}$ values (Fig. 2 (B)).

Estimation of the uptake clearance from in vitro uptake studies using isolated hepatocytes and kidney slices. Time-dependent uptake of drugs was measured in the presence of tracer and excess amount of compounds (For hepatocytes: 0.1 μM and 100 μM for [^{3}H]-pravastatin, [^{3}H]-pitavastatin, [^{3}H]-rosuvastatin, [^{3}H]-valsartan and [^{3}H]-olmesartan; 6.3 μM and 300 μM for [^{14}C]-temocaprilat; 1.7 μM and 1 mM for [^{14}C]-PCG; 10 μM and 1 mM for enalaprilat, benazeprilat, ceftizoxime, and cefmetazole. For kidney slices: 0.1 μM and 1 mM for [^{3}H]-pravastatin; 0.1 μM and 100 μM for [^{3}H]-pitavastatin, [^{3}H]-rosuvastatin, [^{3}H]-valsartan, and [^{3}H]-olmesartan; 6.3 μM and 300 μM for [^{14}C]-temocaprilat; 1.7 μM and 1 mM for [^{14}C]-PCG; 10 μM and 1 mM for enalaprilat, benazeprilat, and cefmetazole; 10 μM and 10 mM for ceftizoxime). All the drugs were taken up linearly into isolated rat hepatocytes within 1 or 2 min and into kidney slices within 15 min under tracer conditions (data not shown). In all cases, the uptake clearance into isolated hepatocytes or kidney slices was decreased in the presence of an excess of compounds, suggesting that their uptake is saturable and mediated by transporters. The uptake clearance of all drugs in isolated hepatocytes and kidney slices is shown in Tables 4 and 5.

Comparison of the intrinsic uptake clearance obtained from integration plot analyses with that from in vitro studies. To examine whether the in vivo intrinsic uptake clearance (P_{1vivo}) obtained from integration plot analyses could be predicted from an in vitro uptake assay (P_{1HEP} for isolated hepatocytes and P_{1KID} for kidney slices), the P_{1vivo} values were compared with the P_{1HEP} and P_{1KID} values (Fig. 3). For this analysis, drugs whose clearance was close to the blood flow (extraction ratio > 0.7) were excluded because the absolute value of blood flow rate sensitively affects the calculated $P_{1,vivo}$ values for these drugs and we cannot obtain the accurate ones. Thus, we didn't use the data of five (pravastatin, pitavastatin, rosuvastatin, temocaprilat and PCG) and four (pravastatin, temocaprilat, benazeprilat and PCG) compounds in the plot for liver and kidney, respectively. In the liver, P_{1vivo} values could be well predicted from in vitro

DMD Fast Forward. Published on April 13, 2009 as DOI: 10.1124/dmd.108.026062
This article has not been copyedited and formatted. The final version may differ from this version.

P_{1HEP} values (Fig. 3 (A)). On the other hand, for kidney, the P_{1vivo} value for each compound was about 10 to 100 times larger than the in vitro P_{1KID} value (Fig. 3 (B)). One of the possible reasons for the discrepancy could be that the drug concentration inside the cells of kidney slices was lower than that in the buffer because a kidney slice consists of multiple cell layers and drugs cannot easily penetrate the multilayered cells, whereas in the physiological condition, drugs can access every cell through blood perfusion. Therefore, the uptake clearance calculated by the uptake amount per unit weight of kidney slice normalized by the drug concentration in the medium might underestimate the true intrinsic uptake clearance. To mimic this situation, we constructed the simple model to explain the relationship between in vitro P_{1KID} and in vivo P_{1vivo} values and estimate the "true" intrinsic uptake clearance ($P_{1KID,corrected}$) based on the results of an in vitro uptake assay using kidney slices (see **Materials and Methods**). Because of analyses using this model, the relationship between P_{1KID} and $P_{1KID,corrected}$ could be described as the following equation by fitting the in vitro P_{1KID} and in vivo P_{1vivo} values for each compound to Equation 23:

$$P_{1KID,corrected} = 32.5 \times P_{1KID} - 7.05 \quad \text{(Eq. 24)}$$

Thus, the $P_{1KID,corrected}$ values were well explained by the P_{1vivo} values and used for the further analyses as an intrinsic uptake clearance in kidney.

Prediction of the organ clearance from in vitro uptake clearance. Based on the intrinsic uptake clearance obtained from in vitro studies (P_{1HEP} and P_{1KID}), the hepatic and renal clearances of all test compounds were calculated by the simple scale-up method and dispersion model. In the case of kidney, $P_{1KID,corrected}$ values instead of P_{1KID} values were used for intrinsic uptake clearance. The predicted organ clearances were compared with the in vivo observed values (Fig. 4). As a result, the hepatic and renal clearance could be predicted from the results of the in vitro uptake assay using isolated hepatocytes and kidney slices, except for the renal clearance of pitavastatin, valsartan, olmesartan, and candesartan, whose renal clearance was relatively small.

DMD Fast Forward. Published on April 13, 2009 as DOI: 10.1124/dmd.108.026062
This article has not been copyedited and formatted. The final version may differ from this version.

Prediction of the elimination routes of drugs from the in vitro uptake assay. Using the predicted hepatic and renal clearances ($CL_{h,predicted}$ and $CL_{r,predicted}$), the fraction excreted into urine (f_{urine}) was calculated by Equation 14 and compared with the observed values. As shown in Figure 5, f_{urine} values for nine compounds could be reasonably predicted from the results of the in vitro assay, but in the case of pitavastatin, valsartan, olmesartan, and candesartan, the predicted f_{urine} values overestimate the real f_{urine} values because of the underestimation of the renal clearances predicted from the in vitro assay.

DMD Fast Forward. Published on April 13, 2009 as DOI: 10.1124/dmd.108.026062
This article has not been copyedited and formatted. The final version may differ from this version.

Discussion

In this study, to demonstrate whether the hepatic and renal clearance of hardly metabolized drugs can be predicted from the results of an in vitro uptake assay using isolated hepatocytes and kidney slices, assuming that the intrinsic uptake clearance approximates the organ intrinsic clearance, we investigated the relationship between the predicted organ clearance calculated from in vivo integration plot analyses and in vitro uptake assays, and the observed organ clearance for 12 drugs in rats. These drugs are anionic at neutral pH and mainly excreted into bile or urine in an unchanged form with minimal metabolism. In addition, these drugs are known to be substrates of drug transporters such as Oatps and Oats.

To examine the importance of the tissue uptake process in the overall clearance of test drugs, the organ clearance ($CL_{bile,B}$ or $CL_{renal,B}$) was compared with the respective uptake clearance measured by integration plot analyses ($CL_{uptake,B,liver}$ or $CL_{uptake,B,kidney}$) in rats. $CL_{bile,B}$ was comparable to $CL_{uptake,B,liver}$, suggesting that the hepatic uptake of compounds was thought to be a determinant factor for overall hepatic clearance (Fig. 2 (A)), while $CL_{renal,B}$ was comparable to $CL_{uptake,B,kidney}$ for 8 drugs, but not for pitavastatin, valsartan, olmesartan, or candesartan (Fig. 2 (B)). The renal clearance of these exceptional drugs was relatively small and underestimates their $CL_{uptake,B,kidney}$ values, suggesting that the uptake process was not a rate-limiting step in their overall renal clearance. Thus, it is possible that backflux from kidney to blood is larger than elimination from kidney to urine, or significant reabsorption from urine to blood is involved in their renal excretion.

Next, to examine whether the in vivo uptake clearance could be predicted from in vitro uptake assays, the intrinsic uptake clearance obtained from integration plot analyses ($P1_{vivo}$) was compared with the in vitro uptake clearance (P_{1HEP} or P_{1KID}) (Fig. 3). P_{1HEP} was almost comparable to $P1_{vivo,liver}$ (Fig. 3 (A)), indicating that hepatic intrinsic uptake clearance can be predicted from in vitro uptake studies. Previous reports have also demonstrated that the in vivo uptake clearance collected using a multiple indicator dilution method and integration plot analysis could be predicted from the in vitro uptake clearance using isolated hepatocytes by simple scale-up calculations (Miyauchi et al., 1993; Kato et al., 1999). On the other hand, because it is difficult to isolate the renal tubular cells, kidney slices are proposed as a good in vitro tool for the characterization of renal uptake. Hasegawa et al. have characterized active uptake of

DMD Fast Forward. Published on April 13, 2009 as DOI: 10.1124/dmd.108.026062
This article has not been copyedited and formatted. The final version may differ from this version.

drugs and established a methodology for examining the contribution of Oat1 and Oat3 to the overall renal uptake of drugs (Hasegawa et al., 2003). However, it remains to be clarified whether the in vivo renal clearance can be predicted using in vitro uptake assays. As a result, $P_{1vivo,kidney}$ was 10 to 100 times larger than P_{1KID} (Fig. 3 (B)). We hypothesized that this apparent discrepancy was caused by the decreased exposure of drugs to the inner cell layer of kidney slices. Then, to determine the theoretical relationship between the apparent uptake clearance per unit weight of kidney slices and true intrinsic clearance, we constructed the simple mathematical model and derived Equation 24 (see **Materials and Methods**). The slope of this equation (32.5) represents half of the number of cell layers in a kidney slice, assuming that the drug-containing buffer can equally access both sides of the kidney slice. The thickness of the kidney slice was about 300 μm and the size of cells is generally 3–10 μm, suggesting that a kidney slice consists of 30–100 cell layers, which is comparable to the estimated number of cell layers. Thus, we corrected the uptake clearance in kidney slices to the "true" intrinsic uptake clearance ($P_{1KID,corrected}$) using Eq. 24.

Finally, in vivo organ clearance was estimated from the results of an in vitro uptake study (Fig. 4). When calculating the organ clearance from intrinsic clearance, we used a dispersion model with a dispersion number (D_N) of 0.17 because a previous report suggested that it is the best prediction method when compared with other models regardless of the magnitude of the clearance (Roberts and Rowland, 1986). The predicted hepatic clearance ($CL_{h,predicted}$) was almost comparable to the observed one ($CL_{bile,B}$) (Fig. 4 (A)), suggesting that the hepatic clearance of compounds could be predicted from the results of the uptake assay using isolated hepatocytes. The renal clearance was calculated in the same way as that of liver using the corrected intrinsic uptake clearance ($P_{1KID,corrected}$). The observed renal clearance ($CL_{renal,B}$) was correlated with the predicted one ($CL_{r,predicted}$) for each drug within a twofold range of difference, except for pitavastatin, valsartan, olmesartan, and candesartan, whose renal clearances were not well predicted from their uptake clearances (Fig. 4 (B)). Moreover, the fraction excreted into urine (f_{urine}) calculated by the predicted organ clearance ($CL_{h,predicted}$ and $CL_{r,predicted}$) was almost comparable to the observed value with the exception of these four compounds (Fig. 5). These results indicated that the absolute values of the organ clearances and the contribution of the liver and kidney to the overall elimination of 8 of 12 substrates could be well predicted from the in vitro uptake studies using isolated hepatocytes and kidney slices. Therefore, the uptake is the rate-limiting step for organ clearance in most

cases and the backflux clearance from organ to blood should be much smaller than the excretion clearance from organ to bile or urine.

Regarding the backflux in the liver, multidrug resistance-associated protein (Mrp) 3 and Mrp4 on the sinusoidal membrane of hepatocytes are involved in the sinusoidal efflux of several glucuronide and sulfate conjugates, and parent compounds such as fexofenadine and methotrexate (Kitamura et al., 2008b; Matsushima et al., 2008; Tian et al., 2008). However, the significance of these transporters on the sinusoidal efflux in humans has not been clarified. Sandwich-cultured hepatocytes enable us to evaluate the sinusoidal efflux and biliary excretion separately, so sandwich-cultured human hepatocytes might provide us with information regarding the relative contribution of backflux and sequestration of drugs (Bi et al., 2006). For reabsorption in the kidney, candidate transporters on the brush border membrane in proximal renal tubular cells have been identified. In rats, Oatp1a1 is reported to be involved in the reabsorption of organic anions such as estradiol-17β-glucuronide and dibromosulfophthalein and their renal clearance was smaller in male rats than in female rats because of its gender-specific expression (Gotoh et al., 2002; Kato et al., 2002). However, in this study, the possible involvement of reabsorption was observed even in female rats, implying the existence of other mechanisms. There is no information regarding the backflux in the kidney to date. Future studies will be needed to clarify the molecular mechanisms of backflux and reabsorption in the kidney. Recently, it has been demonstrated that vectorial transport of drugs could be observed across the monolayer of epithelial cells from the proximal renal tubule seeded onto the culture insert and the expression of several transporters was also confirmed (Lash et al., 2006; Lash et al., 2008). This kind of experimental system may help us investigate bidirectional drug transport in the kidney.

The Oatp family transporters, and Oat1 and Oat3 are mainly involved in the uptake of organic anions in the liver and kidney, respectively. The substrate specificity of Oatp transporters overlaps that of Oat3 such as pravastatin, olmesartan, temocaprilat, and PCG. Thus, the fraction excreted into bile and urine of organic anions may be determined by the relative transport activity of Oatp transporters and Oat3. By comparing the transport activity of transporter-specific ligands or relative expression level in organ samples and transporter-expression systems, the major elimination route of drugs can be estimated from the relative transport activity in each expression system. In this study, we selected minimally metabolized compounds

for analysis. Recent reports have suggested the importance of uptake transporters in the hepatic clearance of some drugs such as repaglinide, bosentan, and atorvastatin, which are extensively metabolized by CYP enzymes (Shitara et al., 2006). Even in the case of extensively metabolized drugs, if uptake process is mediated by transporters, this prediction method may be applied for these substrates because the hepatic clearance may be solely determined by the uptake clearance.

To predict the human pharmacokinetics, human cryopreserved hepatocytes and kidney slices are now available and have been used in the characterization of the contribution of uptake transporters to the overall uptake of drugs and drug–drug interactions (Hirano et al., 2004; Nozaki et al., 2004). Using the same approach, we will be able to predict the elimination route of drugs in humans using in vitro uptake assays.

In summary, absolute values of hepatic and renal clearances and the fraction excreted in urine can be predicted for minimally metabolized drugs from in vitro uptake studies using isolated hepatocytes and kidney slices, except for drugs whose renal clearance was relatively small. Although further studies are needed for more accurate prediction, this model will be applicable to drug screening for the prediction of organ clearance and the distribution of compounds in the liver and kidney.

DMD Fast Forward. Published on April 13, 2009 as DOI: 10.1124/dmd.108.026062
This article has not been copyedited and formatted. The final version may differ from this version.

Acknowledgments

We express our great appreciation to Daiichi-Sankyo Co. (Tokyo, Japan) for providing us with [^{3}H]-pravastatin, [^{3}H]-olmesartan, [^{14}C]-temocaprilat, and unlabeled pravastatin, olmesartan, and temocaprilat; Novartis Pharma (Basel, Switzerland) for providing us with [^{3}H]-labeled and unlabeled valsartan; Kowa Co. (Tokyo, Japan) for providing us with [^{3}H]-labeled and unlabeled pitavastatin; and AstraZeneca (London, UK) for providing us with [^{3}H]-labeled and unlabeled rosuvastatin. We thank Dr. Junko Iida and Mr. Futoshi Kurotobi (Shimadzu, Kyoto, Japan) for technical support of the LC/MS system.

References

Balani SK, Miwa GT, Gan LS, Wu JT and Lee FW (2005) Strategy of utilizing in vitro and in vivo ADME tools for lead optimization and drug candidate selection. *Curr Top Med Chem* **5**:1033-1038.

Bi YA, Kazolias D and Duignan DB (2006) Use of cryopreserved human hepatocytes in sandwich culture to measure hepatobiliary transport. *Drug Metab Dispos* **34**:1658-1665.

Davies B and Morris T (1993) Physiological parameters in laboratory animals and humans. *Pharm Res* **10**:1093-1095.

Gotoh Y, Kato Y, Stieger B, Meier PJ and Sugiyama Y (2002) Gender difference in the Oatp1-mediated tubular reabsorption of estradiol 17beta-D-glucuronide in rats. *Am J Physiol Endocrinol Metab* **282**:E1245-1254.

Hasegawa M, Kusuhara H, Endou H and Sugiyama Y (2003) Contribution of organic anion transporters to the renal uptake of anionic compounds and nucleoside derivatives in rat. *J Pharmacol Exp Ther* **305**:1087-1097.

Hasegawa M, Kusuhara H, Sugiyama D, Ito K, Ueda S, Endou H and Sugiyama Y (2002) Functional involvement of rat organic anion transporter 3 (rOat3; Slc22a8) in the renal uptake of organic anions. *J Pharmacol Exp Ther* **300**:746-753.

Hirano M, Maeda K, Shitara Y and Sugiyama Y (2004) Contribution of OATP2 (OATP1B1) and OATP8 (OATP1B3) to the hepatic uptake of pitavastatin in humans. *J Pharmacol Exp Ther* **311**:139-146.

Ieiri I, Takane H, Hirota T, Otsubo K and Higuchi S (2006) Genetic polymorphisms of drug transporters: pharmacokinetic and pharmacodynamic consequences in pharmacotherapy. *Expert Opin Drug Metab Toxicol* **2**:651-674.

Ishizuka H, Konno K, Naganuma H, Nishimura K, Kouzuki H, Suzuki H, Stieger B, Meier PJ and Sugiyama Y (1998) Transport of temocaprilat into rat hepatocytes: role of organic anion transporting polypeptide. *J Pharmacol Exp Ther* **287**:37-42.

Ishizuka H, Konno K, Naganuma H, Sasahara K, Kawahara Y, Niinuma K, Suzuki H and Sugiyama Y (1997) Temocaprilat, a novel angiotensin-converting enzyme inhibitor, is excreted in bile via an ATP-dependent active transporter (cMOAT) that is deficient in Eisai hyperbilirubinemic mutant rats (EHBR). *J Pharmacol Exp Ther* **280**:1304-1311.

Ito K, Suzuki H, Horie T and Sugiyama Y (2005) Apical/basolateral surface expression of drug transporters and its role in vectorial drug transport. *Pharm Res* **22**:1559-1577.

Iwatsubo T, Hirota N, Ooie T, Suzuki H and Sugiyama Y (1996) Prediction of in vivo drug disposition from in vitro data based on physiological pharmacokinetics. *Biopharm Drug Dispos* **17**:273-310.

Kato Y, Akhteruzzaman S, Hisaka A and Sugiyama Y (1999) Hepatobiliary transport governs overall elimination of peptidic endothelin antagonists in rats. *J Pharmacol Exp Ther* **288**:568-574.

Kato Y, Kuge K, Kusuhara H, Meier PJ and Sugiyama Y (2002) Gender difference in the urinary excretion of organic anions in rats. *J Pharmacol Exp Ther* **302**:483-489.

Kitamura S, Maeda K and Sugiyama Y (2008a) Recent progresses in the experimental methods and evaluation strategies of transporter functions for the prediction of the pharmacokinetics in humans. *Naunyn Schmiedebergs Arch Pharmacol* **377**:617-628.

Kitamura Y, Hirouchi M, Kusuhara H, Schuetz JD and Sugiyama Y (2008b) Increasing systemic exposure of methotrexate by active efflux mediated by multidrug resistance-associated protein 3 (Mrp3/Abcc3). *J Pharmacol Exp Ther*.

Konig J, Seithel A, Gradhand U and Fromm MF (2006) Pharmacogenomics of human OATP transporters. *Naunyn Schmiedebergs Arch Pharmacol* **372**:432-443.

Lash LH, Putt DA and Cai H (2006) Membrane transport function in primary cultures of human proximal tubular cells. *Toxicology* **228**:200-218.

Lash LH, Putt DA and Cai H (2008) Drug metabolism enzyme expression and activity in primary cultures of human proximal tubular cells. *Toxicology* **244**:56-65.

Lynch T and Price A (2007) The effect of cytochrome P450 metabolism on drug response, interactions, and adverse effects. *Am Fam Physician* **76**:391-396.

Matsushima S, Maeda K, Hayashi H, Debori Y, Schinkel AH, Schuetz JD, Kusuhara H and Sugiyama Y (2008) Involvement of multiple efflux transporters in hepatic disposition of fexofenadine. *Mol Pharmacol* **73**:1474-1483.

Miyauchi S, Sawada Y, Iga T, Hanano M and Sugiyama Y (1993) Comparison of the hepatic uptake clearances of fifteen drugs with a wide range of membrane permeabilities in isolated rat hepatocytes and perfused rat livers. *Pharm Res* **10**:434-440.

Nozaki Y, Kusuhara H, Endou H and Sugiyama Y (2004) Quantitative evaluation of the drug-drug interactions between methotrexate and nonsteroidal anti-inflammatory drugs in the renal uptake process based on the contribution of organic anion transporters and reduced folate carrier. *J Pharmacol Exp Ther* **309**:226-234.

Oguchi H, Miyasaka M, Koiwai T, Tokunaga S, Hora K, Sato K, Yoshie T, Shioya H and Furuta S (1993) Pharmacokinetics of temocapril and enalapril in patients with various degrees of renal insufficiency. *Clin Pharmacokinet* **24**:421-427.

Roberts MS and Rowland M (1986) Correlation between in-vitro microsomal enzyme activity and whole organ hepatic elimination kinetics: analysis with a dispersion model. *J Pharm Pharmacol* **38**:177-181.

Roberts SA (2001) High-throughput screening approaches for investigating drug metabolism and pharmacokinetics. *Xenobiotica* **31**:557-589.

Shitara Y, Horie T and Sugiyama Y (2006) Transporters as a determinant of drug clearance and tissue distribution. *Eur J Pharm Sci* **27**:425-446.

Shitara Y, Sato H and Sugiyama Y (2005) Evaluation of drug-drug interaction in the hepatobiliary and renal transport of drugs. *Annu Rev Pharmacol Toxicol* **45**:689-723.

Tian X, Swift B, Zamek-Gliszczynski MJ, Belinsky MG, Kruh GD and Brouwer KL (2008) Impact of basolateral multidrug resistance-associated protein (Mrp) 3 and Mrp4 on the hepatobiliary disposition of fexofenadine in perfused mouse livers. *Drug Metab Dispos* **36**:911-915.

Tsuji A (2006) Impact of transporter-mediated drug absorption, distribution, elimination and drug interactions in antimicrobial chemotherapy. *J Infect Chemother* **12**:241-250.

Yamaoka K, Tanigawara Y, Nakagawa T and Uno T (1981) A pharmacokinetic analysis program (multi) for microcomputer. *J Pharmacobiodyn* **4**:879-885.

Yamazaki M, Suzuki H, Hanano M, Tokui T, Komai T and Sugiyama Y (1993) Na(+)-independent multispecific anion transporter mediates active transport of pravastatin into rat liver. *Am J Physiol* **264**:G36-44.

Footnotes

This study was supported by a Research Grant (Development of Technology to Create Research Model Cells) from the New Energy and Industrial Technology Development Organization (NEDO) of Japan and a Grant-in-Aid for Young Scientists (B) (19790119) from the Ministry of Education, Culture, Sports, Science and Technology.

Legends for figures

Figure 1. A simple mathematical model for considering the permeation of drugs in kidney slices.

The relationship between the "true" intrinsic uptake clearance ($P_{1KID,corrected}$) and the observed uptake clearance in kidney slices (P_{1KID}) was theoretically explained by the simple mathematical model as shown in this figure. The details are described in the **Materials and Methods** section.

Figure 2. Comparison between in vivo organ clearance ($CL_{bile,B}$ and $CL_{renal,B}$) and organ uptake clearance ($CL_{uptake,B,liver}$ and $CL_{uptake,B,kidney}$) in liver and kidney.

$CL_{uptake,B}$ values for the liver and kidney were obtained from integration plot analyses. $CL_{bile,B}$ and $CL_{uptake,B,liver}$ (for the liver) are plotted in (A), and $CL_{renal,B}$ and $CL_{uptake,B,kidney}$ (for the kidney) are plotted in (B). The enlarged view of (B) (range of X-axis and Y-axis: 1–100 mL/min/kg; plots inside the circle) is shown in (C). Plots represent: 1, pravastatin; 2, pitavastatin; 3, rosuvastatin; 4, valsartan; 5, olmesartan; 6, candesartan; 7, temocaprilat; 8, enalaprilat; 9, benazeprilat; 10, PCG; 11, ceftizoxime; and 12, cefmetazole. The solid line represents the line of unity and the dashed lines the lines of 1:2 and 2:1 correlations.

Figure 3. Comparison between in vivo intrinsic uptake clearance (P_{1vivo}) and in vitro intrinsic uptake clearance (P_{1HEP} and P_{1KID}) in liver and kidney.

P_{1vivo} values were calculated from $CL_{uptake,B}$ values obtained from integration plot analyses. $P_{1vivo,liver}$ and P_{1HEP} values (for the liver) are plotted in (A), and $P_{1vivo,kidney}$ and P_{1KID} values (for the kidney) are plotted in (B). (A) The solid line represents the line of unity and the dashed lines the lines of 1:2 and 2:1 correlations. (B) The solid curve represents the theoretical value calculated from Equation 24 derived from the simple mathematical model (see **Materials and Methods**). The solid line represents the line of unity and the dashed lines the lines of 1:10 and 1:100 correlations as indicated. Plots represent: 1, pravastatin; 2, pitavastatin; 3, rosuvastatin; 4, valsartan; 5, olmesartan; 6, candesartan; 7, temocaprilat; 8, enalaprilat; 9, benazeprilat; 10, PCG; 11, ceftizoxime; and 12, cefmetazole. Please note that 1, 2, 3, 7, and 10, and 1, 7, 9, and 10 were not plotted in Figure 3(A) and (B), respectively because we cannot obtain the accurate P1,vivo values for drugs with high extraction ratio (>0.7). The details are described in the **Results** section.

DMD Fast Forward. Published on April 13, 2009 as DOI: 10.1124/dmd.108.026062
This article has not been copyedited and formatted. The final version may differ from this version.

Figure 4. Comparison between the observed ($CL_{bile,B}$ and $CL_{renal,B}$) and the predicted organ clearance ($CL_{h,predicted}$ and $CL_{r,predicted}$) in liver and kidney.

$CL_{h,predicted}$ and $CL_{r,predicted}$ were calculated based on Equations 9–12, assuming that uptake clearance obtained from rat-isolated hepatocytes and kidney slices was equal to the intrinsic clearance in each organ (CL_{int}). For calculation of $CL_{r,predicted}$, the "true" intrinsic uptake clearance ($P_{1KID,corrected}$), corrected based on the simple model analysis to explain the relationship between in vitro P_{1KID} and in vivo P_{1vivo} values, was used. The details are described in the **Materials and Methods** section. $CL_{bile,B}$ and $CL_{h,predicted}$ (for the liver) are plotted in (A), and $CL_{renal,B}$ and $CL_{r,predicted}$ (for the kidney) are plotted in (B). The enlarged view of (B) (range of X-axis and Y-axis: 1–100 mL/min/kg; plots inside the circle) is shown in (C). Plots represent: 1, pravastatin; 2, pitavastatin; 3, rosuvastatin; 4, valsartan; 5, olmesartan; 6, candesartan; 7, temocaprilat; 8, enalaprilat; 9, benazeprilat; 10, PCG; 11, ceftizoxime; and 12, cefmetazole. The solid line and the dashed lines represent the line of unity and the lines of 1:2 and 2:1 correlations.

Figure 5. Comparison between the observed and the predicted fraction excreted into urine (f_{urine}) of 12 compounds in female SD rats.

The fraction excreted into urine (f_{urine}) was predicted by Eq. 14 using $CL_{h,predicted}$ and $CL_{r,predicted}$ values. The predicted and observed fractions excreted into urine are plotted. Plots represent: 1, pravastatin; 2, pitavastatin; 3, rosuvastatin; 4, valsartan; 5, olmesartan; 6, candesartan; 7, temocaprilat; 8, enalaprilat; 9, benazeprilat; 10, PCG; 11, ceftizoxime; and 12, cefmetazole. The solid line represents the line of unity.

Table 1. Pharmacokinetic parameters of 12 drugs in female SD rats.

Female SD rats received a bolus intravenous administration of pitavastatin (0.2 mg/kg), rosuvastatin (0.5 mg/kg), valsartan (0.5 mg/kg), olmesartan (0.08 mg/kg), candesartan (0.08 mg/kg), temocaprilat (0.5 mg/kg), enalaprilat (0.5 mg/kg), benazeprilat (0.5 mg/kg), PCG (2 mg/kg), and ceftizoxime (1 mg/kg) or constant infusion of pravastatin (76 mg/min/kg after intravenous administration of 0.67 mg/kg) and cefmetazole (0.1 mg/min/kg). The concentrations of drugs in plasma, bile, and urine were measured and pharmacokinetic parameters were calculated. Each value is expressed as mean ± S.E. of 4–5 rats. $CL_{tot,B}$: total clearance based on the drug concentration in blood; $CL_{bile,B}$: biliary clearance based on the drug concentration in blood; $CL_{renal,B}$: renal clearance based on the drug concentration in blood; f_{bile}: fraction excreted into bile; f_{urine}: fraction excreted into urine. No. for each compound corresponds to the numerical coding attached to each plot in all the figures.

No	Compound	$CL_{tot,B}$			$CL_{bile,B}$			$CL_{renal,B}$			f_{bile}			f_{urine}		
		mL/min/kg									% of dose					
1	Pravastatin	123	±	15	78.3	±	6.0	32.5	±	5.2	65.8	±	4.8	26.0	±	1.6
2	Pitavastatin	17.8	±	2.4	12.2	±	1.7	0.0108	±	0.0011	63.8	±	2.3	0.0564	±	0.0236
3	Rosuvastatin	127	±	7	111	±	5	8.42	±	2.09	83.9	±	2.5	6.34	±	1.61
4	Valsartan	22.3	±	1.3	16.0	±	0.7	0.405	±	0.171	81.5	±	2.9	1.86	±	1.39
5	Olmesartan	3.83	±	0.47	2.99	±	0.45	0.0238	±	0.0023	86.8	±	3.4	0.587	±	0.090
6	Candesartan	4.14	±	0.23	3.03	±	0.24	0.200	±	0.019	73.6	±	3.1	4.94	±	0.58
7	Temocaprilat	53.0	±	1.0	34.4	±	2.6	7.81	±	1.04	72.7	±	4.2	16.5	±	2.1
8	Enalaprilat	22.8	±	2.5	2.96	±	0.32	17.4	±	2.1	13.4	±	0.1	76.1	±	3.4
9	Benazeprilat	46.1	±	3.5	20.2	±	2.9	24.0	±	0.8	43.7	±	6.6	53.0	±	4.8
10	PCG	62.4	±	1.7	8.66	±	1.10	42.6	±	1.3	14.4	±	1.8	71.1	±	2.6
11	Ceftizoxime	23.3	±	2.9	1.21	±	0.16	19.5	±	1.8	5.32	±	0.18	86.2	±	3.5
12	Cefmetazole	54.3	±	5.2	24.2	±	2.1	24.0	±	1.4	46.7	±	8.1	45.5	±	5.7

DMD Fast Forward. Published on April 13, 2009 as DOI: 10.1124/dmd.108.026062
This article has not been copyedited and formatted. The final version may differ from this version.

Table 2. Blood-to-plasma concentration ratio (R_B) and protein unbound fraction in plasma (f_u) and in blood (f_B) for each compound in female SD rats.

f_u and R_B values were measured and f_B was calculated by dividing f_u by R_B. Each value is expressed as mean ± S.E. of triplicate determinations. f_u: protein unbound fraction in plasma; R_B: blood-to-plasma concentration ratio; f_B: protein unbound fraction in blood (= f_u / R_B).

Compound	f_u			R_B			f_B		
Pravastatin	0.509	±	0.047	0.769	±	0.038	0.662	±	0.069
Pitavastatin	0.00642	±	0.00174	0.539	±	0.012	0.012	±	0.003
Rosuvastatin	0.0525	±	0.0058	0.631	±	0.029	0.083	±	0.010
Valsartan	0.0100	±	0.0008	0.702	±	0.059	0.014	±	0.002
Olmesartan	0.00861	±	0.00067	0.843	±	0.02	0.010	±	0.001
Candesartan	0.00651	±	0.00150	0.578	±	0.02	0.011	±	0.003
Temocaprilat	0.0639	±	0.0099	0.780	±	0.055	0.082	±	0.014
Enalaprilat	0.420	±	0.003	0.751	±	0.010	0.559	±	0.008
Benazeprilat	0.245	±	0.076	0.670	±	0.042	0.366	±	0.116
PCG	0.454	±	0.085	0.664	±	0.014	0.684	±	0.129
Ceftizoxime	0.654	±	0.070	0.767	±	0.032	0.853	±	0.098
Cefmetazole	0.598	±	0.063	0.691	±	0.021	0.865	±	0.095

DMD Fast Forward. Published on April 13, 2009 as DOI: 10.1124/dmd.108.026062
This article has not been copyedited and formatted. The final version may differ from this version.

Table 3. Tissue uptake clearance of drugs obtained from integration plot analyses.

$CL_{uptake,p}$ (ml/min/g tissue) obtained from the slope of an integration plot was converted to $CL_{uptake,B}$ (mL/min/kg) using the weight of rat liver (38.3 g liver per kg body weight) and kidney (7.27 g kidney per kg body weight), and R_B values. Each value is expressed as mean ± computer-calculated S.D. of 3–4 rats. $CL_{uptake,B}$: tissue uptake clearance based on the drug concentration in blood.

Compound	$CL_{uptake,B}$ mL/min/kg					
	liver			kidney		
Pravastatin	57.3	±	9.4	27.1	±	3.5
Pitavastatin	63.7	±	1.3	13.9	±	0.3
Rosuvastatin	66.1	±	9.5	20.9	±	1.2
Valsartan	33.3	±	3.6	3.50	±	0.53
Olmesartan	13.7	±	0.3	2.46	±	0.52
Candesartan	6.18	±	1.52	0.932	±	0.206
Temocaprilat	45.6	±	0.9	20.5	±	0.7
Enalaprilat	4.54	±	0.75	18.7	±	1.8
Benazeprilat	16.0	±	2.0	29.2	±	0.8
PCG	49.7	±	3.3	44.8	±	11.5
Ceftizoxime	2.89	±	0.03	12.3	±	1.1
Cefmetazole	37.6	±	1.2	47.2	±	0.3

DMD Fast Forward. Published on April 13, 2009 as DOI: 10.1124/dmd.108.026062
This article has not been copyedited and formatted. The final version may differ from this version.

Table 4. Uptake clearance of drugs in rat isolated hepatocytes.

Time-dependent uptake of drugs in rat isolated hepatocytes was measured in the presence of tracer amount of drugs in the incubation buffer (0.1 μM for [^{3}H]-pravastatin, [^{3}H]-pitavastatin, [^{3}H]-rosuvastatin, [^{3}H]-valsartan, and [^{3}H]-olmesartan; 6.3 μM for [^{14}C]-temocaprilat; 1.7 μM for [^{14}C]-PCG; 10 μM for enalaprilat, benazeprilat, ceftizoxime, and cefmetazole). The in vitro intrinsic uptake clearance (P_{1hep}) was calculated by dividing initial uptake velocity by the drug concentration in the incubation buffer. Each value is expressed as mean ± S.E. of triplicate determinations.

Compound	P_{1hep} μL/min/10^6 cells		
Pravastatin	34.3	±	4.3
Pitavastatin	519	±	9
Rosuvastatin	201	±	20
Valsartan	112	±	15
Olmesartan	45.2	±	11.3
Candesartan	72.5	±	3.1
Temocaprilat	18.6	±	1.1
Enalaprilat	1.19	±	0.78
Benazeprilat	4.70	±	0.70
PCG	8.77	±	2.26
Ceftizoxime	1.30	±	0.20
Cefmetazole	19.9	±	5.1

DMD Fast Forward. Published on April 13, 2009 as DOI: 10.1124/dmd.108.026062
This article has not been copyedited and formatted. The final version may differ from this version.

Table 5. Uptake clearance of drugs in rat kidney slices.

Time-dependent uptake of drugs into rat kidney slices was measured in the presence of tracer amount of drugs in the incubation buffer (0.1 μM for [^{3}H]-pravastatin, [^{3}H]-pitavastatin, [^{3}H]-rosuvastatin, [^{3}H]-valsartan, and [^{3}H]-olmesartan; 6.3 μM for [^{14}C]-temocaprilat; 1.7 μM for [^{14}C]-PCG; 10 μM for enalaprilat, benazeprilat, cefmetazole, and ceftizoxime). The in vitro intrinsic uptake clearance (P_{1kid}) was calculated by dividing initial uptake velocity by the drug concentration in the incubation buffer. Each value is expressed as mean ± S.E. of triplicate determinations.

Compound	P_{1kid} mL/min/g kidney		
Pravastatin	0.236	±	0.110
Pitavastatin	0.912	±	0.173
Rosuvastatin	0.310	±	0.110
Valsartan	1.21	±	0.29
Olmesartan	0.644	±	0.175
Candesartan	0.796	±	0.363
Temocaprilat	0.290	±	0.115
Enalaprilat	0.220	±	0.135
Benazeprilat	0.122	±	0.047
PCG	0.521	±	0.106
Ceftizoxime	0.0415	±	0.0272
Cefmetazole	0.0953	±	0.0176

DMD Fast Forward. Published on April 13, 2009 as DOI: 10.1124/dmd.108.026062
This article has not been copyedited and formatted. The final version may differ from this version.

Fig. 1

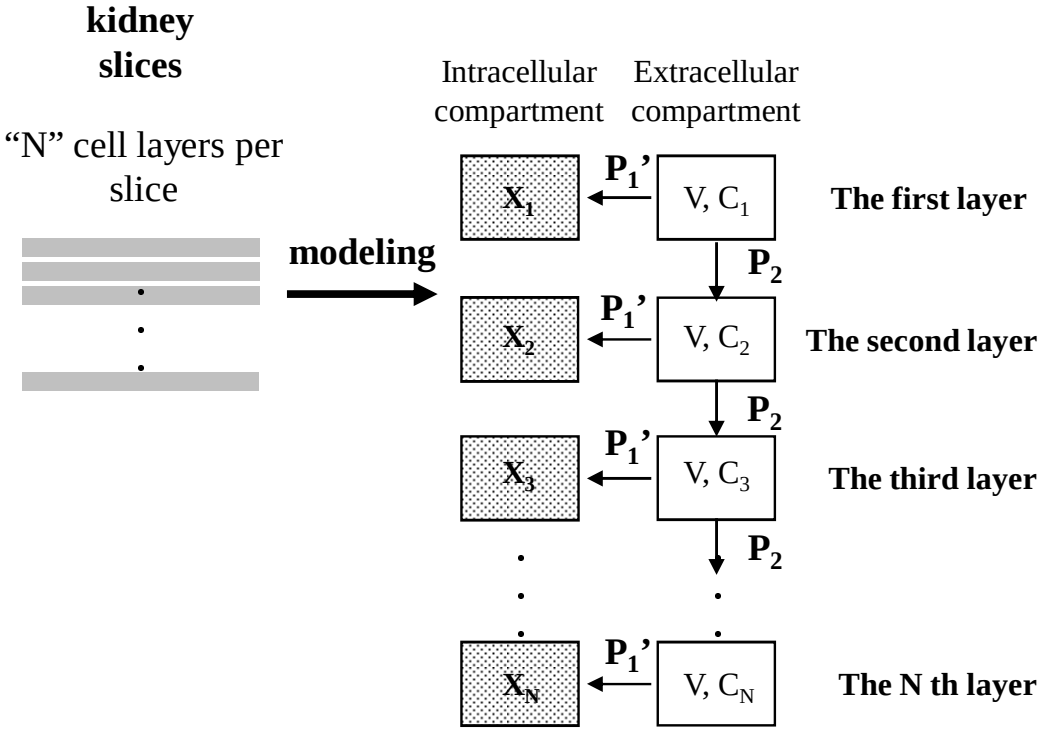

DMD Fast Forward. Published on April 13, 2009 as DOI: 10.1124/dmd.108.026062
This article has not been copyedited and formatted. The final version may differ from this version.

Fig. 2

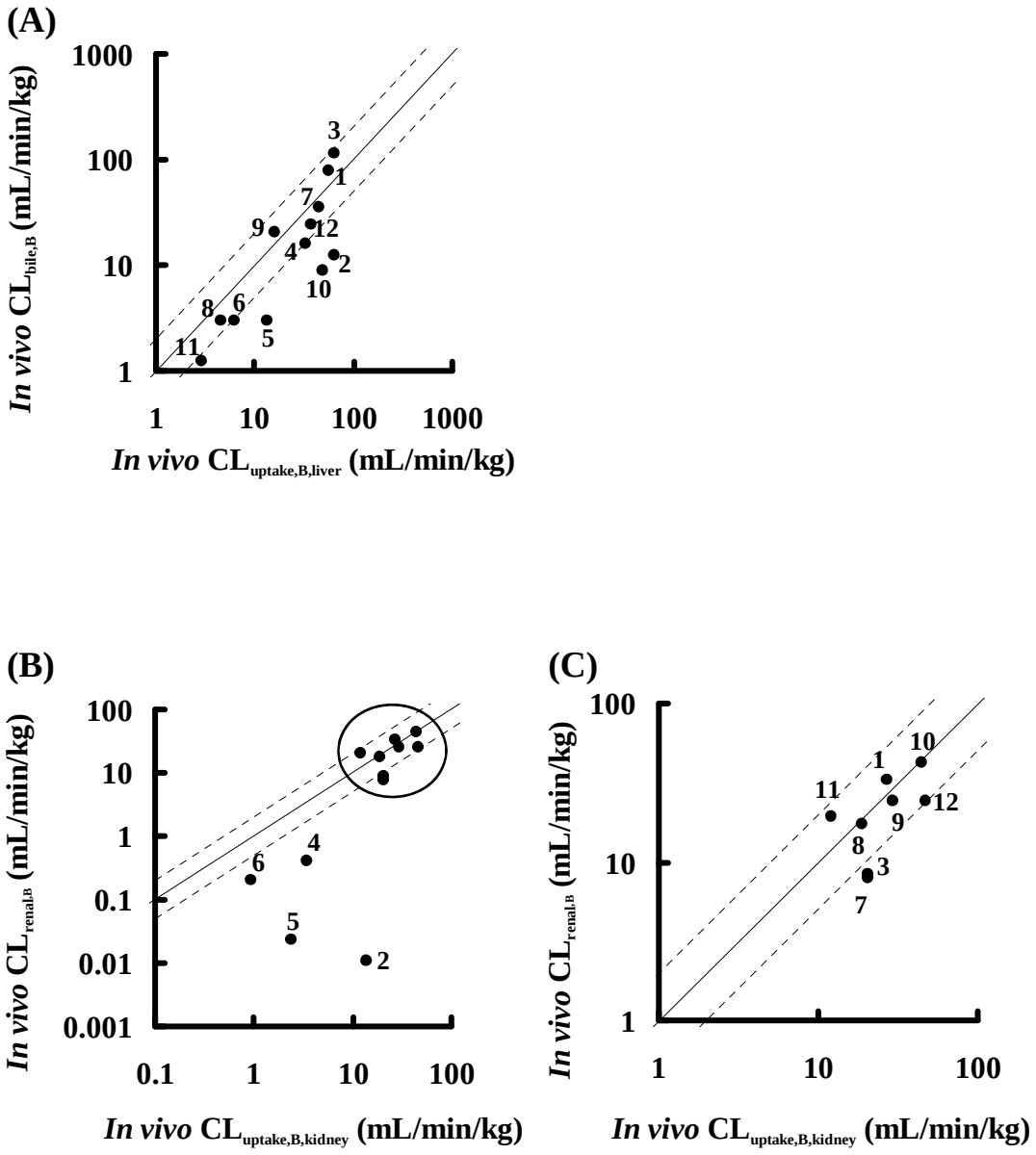

DMD Fast Forward. Published on April 13, 2009 as DOI: 10.1124/dmd.108.026062
This article has not been copyedited and formatted. The final version may differ from this version.

Fig. 3

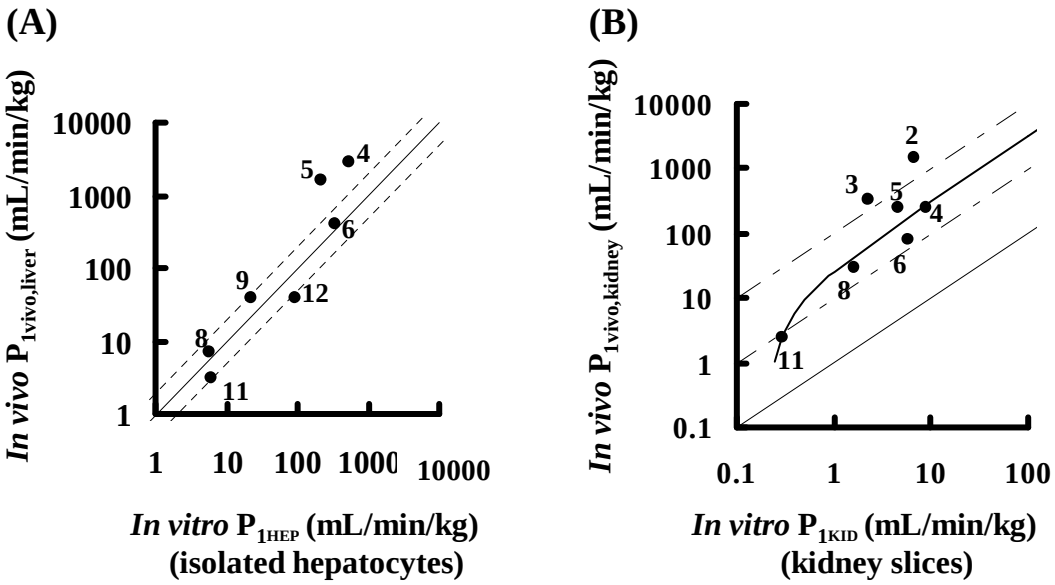

DMD Fast Forward. Published on April 13, 2009 as DOI: 10.1124/dmd.108.026062
This article has not been copyedited and formatted. The final version may differ from this version.

Fig. 4

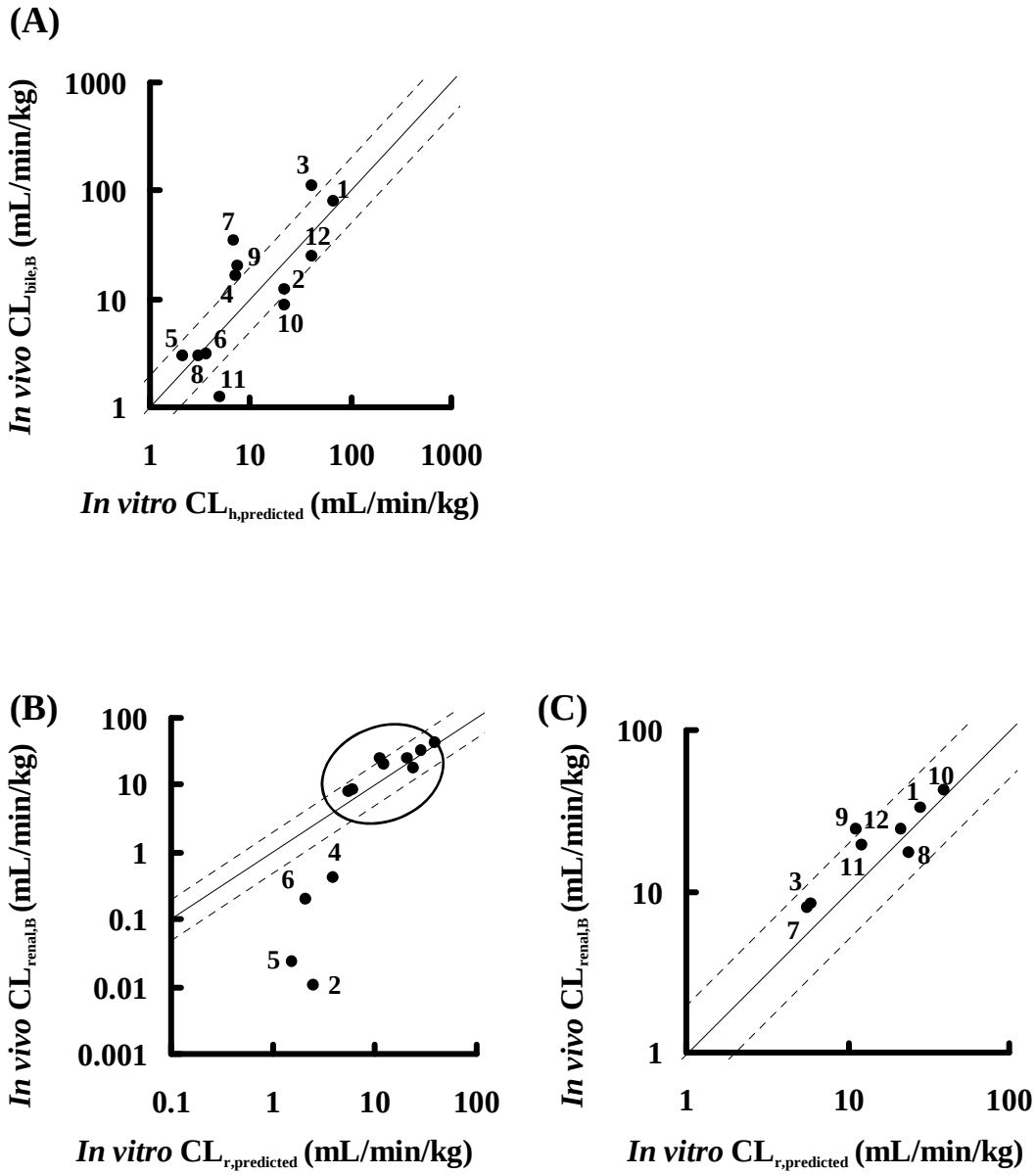

DMD Fast Forward. Published on April 13, 2009 as DOI: 10.1124/dmd.108.026062
This article has not been copyedited and formatted. The final version may differ from this version.

Fig. 5